T.E.S.T.

Team Results Document

T.E.S.T. 2020, August 13th

Supervisor and Coaches
dr. Leo van IJzendoorn
ing. Claudia Schot
ir. Rafiq Lubken

Team Members
Maurits van der Vorm
Thomas Stekelenburg
Leandra Vermeulen
Caitlin Pieneman
Ernst Paul Swens
Eveline Nugraha
Imke Rodenburg
Melle Houben
Jesse Jägers
Mirre Trines

tuetest.nl
info@tuetest.nl
Eindhoven University of Technology

Summary

Valproic acid (VPA) is an anti-epileptic drug (AED) of which the majority is bound (bVPA) to serum proteins, mainly albumin. In order to measure the unbound and pharmacologically active fraction of VPA (fVPA) in blood, a filtration step and a molecular recognition step are needed.

We as the T. E. S. T. student team developed a cartridge and a reader. The filtration step uses magnetic beads coated with anti-albumin antibodies to extrude albumin and bVPA from a blood sample. The molecular recognition that follows uses a bioluminescent competitive immunoassay. The assay uses anti-VPA antibodies and a VPA-analogue that when combined produce a blue light signal. To correct for environmental factors that might influence the light-producing enzyme, a similar enzyme that produces green light is used as a reference signal. The filtration and molecular recognition are located in a centrifugal cartridge that is easy to use and only requires a single drop of blood. Within a few minutes after placing the cartridge in the reader the fVPA concentration will be displayed in the supportive mobile app. The regular use of this device to measure fVPA concentrations by epilepsy patients will help medical doctors to give the right dosage of VPA and possibly other AEDs in the future.

Table of Content

1. Biosensor System and Assay

Valproic acid (VPA) is a small fatty acid used for treatment of epilepsy of which the majority is bound to serum proteins, mainly albumin. In order to measure the unbound pharmacologically active fraction of VPA in blood a filtration step and a molecular recognition step are needed. We have designed a reader and cartridge which incorporates both of these steps. The filtration and molecular recognition methods will be explained in the first section, followed by the cartridge design, physical transduction and reader technology and user interaction.

1.1. Molecular recognition and assay reagents

1.1.1 Filtration

Based on the assumption that anti-VPA antibodies recognize both VPA bound to albumin (bVPA) and free VPA (fVPA), the total VPA concentration can be measured by the assay without a filtration step. To determine only the fVPA concentration, a separation technique is introduced to extrude albumin and bVPA from fVPA via magnetic separation (Fig. 1.1A), inspired by PureProteome™ [1]. Magnetic particles (Dynabeads™ Protein G, Thermo Fisher Scientific) functionalized with anti-albumin monoclonal antibodies (EPR20195, Abcam) in solution are added to the plasma sample containing albumin and VPA. The plasma sample and solution are mixed using the magnetic properties of the particles and a changing magnetic field. It is assumed that the anti-albumin antibodies on the magnetic particles bind to both the albumin and VPA-albumin complex. After reaching equilibrium, the magnetic particles are isolated from the solution by magnetic separation. The solution containing the remaining fVPA will flow to the assay chamber.

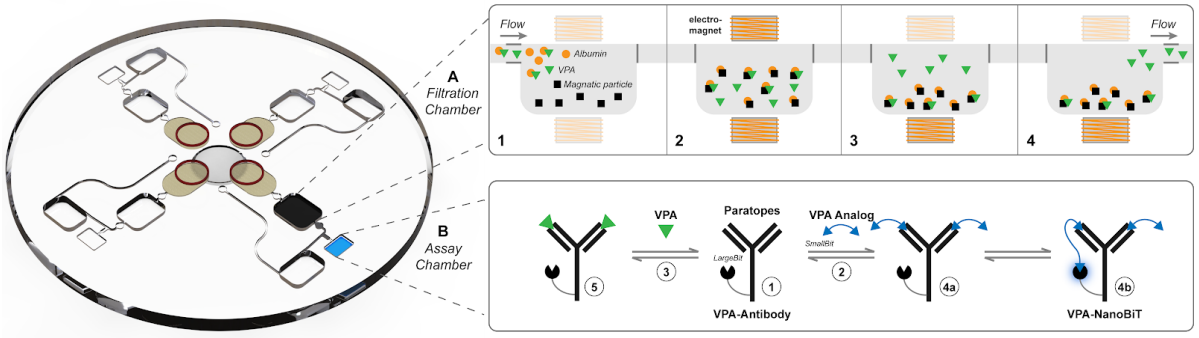

Fig. 1.1. A *Filtration Chamber 1) Sample is introduced in the filtration chamber; 2) Sample and solution are magnetically mixed until equilibrium is reached; 3) Magnetic particles are isolated; 4) Solution containing fVPA flows to the assay chamber.*
B *Assay Chamber 1) VPA-Antibody with LargeBiT (VPA-Ab) 2) VPA analogue with SmallBiT (VPAa) 3) Free VPA (fVPA) 4a) VPAa coupled to VPA-Ab 4b) Formation of VPA-NanoBiT (VPA-NB) 5) VPA-Ab bound to fVPA*

1.1.2 Assay

For the detection of fVPA, we propose a bioluminescent competitive immunoassay inspired by the cloned enzyme donor immunoassay (CEDIA) [2] while substituting the luminescent enzyme by the small, stable and bright NanoLuc enzyme [3]. This lowers the detection limit of the assay. The assay comprises two major components: A VPA analogue coupled to a split enzyme (VPAa) and an anti-VPA antibody coupled to a split enzyme (VPA-Ab).

In the assay chamber, a competition between VPAa and fVPA will occur on the paratope of a Valproic Acid Monoclonal Antibody (VP10-115.2, Thermo Fisher Scientific), (Fig. 1.1B). To create a signal that depends on the amount of fVPA, a split reporter enzyme NanoBiT is added [4]. NanoBit is an engineered complementation reporter enzyme based on nano luciferase (NanoLuc) which consists of two peptides: SmallBiT (1.3 kDa) and LargeBiT (18 kDa). The binding of these two components leads to the formation of the complete bioluminescent enzyme NanoBit. This complex catalyzes the oxidation of the substrate furimazine into furamidine, thereby emitting a photon with a wavelength of 460 nm.

The molecular recognition and the optical signal are coupled by the conjugation of SmallBiT and LargeBiT to VPAa and VPA-Ab, respectively. The conjugation of these components enables NanoBiT formation (VPA-NB) that is favored when SmallBiT and LargeBiT are in close proximity, which occurs when VPAa is bound to VPA-Ab (Fig. 1.1B complex 4a, 4b). As fVPA and VPAa compete for binding to VPA-Ab, a signal is created that is inversely proportional to the fVPA concentration.

VPAa is chemically engineered with an aminated analog of VPA, 6-amino-2-propylhexanoic acid (ENA444724622 Enamine, Merck). This analog forms the basis for solid phase peptide synthesis where a semi-flexible glycine-serine linker attached to SmallBiT will be formed on the aminated site. VPA-Ab is

synthesized by attaching LargeBiT to the anti-VPA antibody using LASIC-technology [5]. LASIC is based on a non-covalent binding of protein A to the Fc region of the anti-VPA antibody. The non-covalent bond will be covalently crosslinked via activation of a photoreactive non-natural amino acid benzoylphenylalanine (BPA) with UV-light. By recombinant protein expression of the LargeBiT and a glycine-serine linker in combination with protein Z containing BPA, the VPA-Ab will be formed.

The final component of the assay is the NanoLuc-mNeonGreen protein (NLNG), a BRET-based protein with a 95% BRET efficiency that produces a green emission peak at 517 nm [6]. Both NLNG and VPA-NB include NanoBit, and therefore have identical enzymatic activity regardless of environmental conditions, such as pH, temperature and substrate concentration. The absolute light intensity produced by both VPA-Ab and NLNG can fluctuate between experiments, whereas the ratio between blue emission and green emission peaks only depends on the VPA concentration. This ratiometric measuring component corrects for experimental inconsistencies, increasing the robustness of the fVPA measurement.

1.2. Cartridge technology

The cartridge is based on compact disk (CD)- centrifugal microfluidics. This design allows control of the fluidics through passive valves, which is required for a separation between the filtration and assay step. These valves have a simple geometry and do not require local surface modifications or actuators, easing the production process for mass production. Additionally, no outside pressure nor tubing is required, increasing the robustness of the biosensor and the ability to be used in a point-of-care device. The disk can be fabricated easily and cheaply from PDMS using soft lithography [7] [8] [9].

Blood placed at the inlet first enters the cartridge through a filter [10] in which the blood cells remain behind (Fig. 1.2). By centrifugal forces the plasma flows into the filtration chamber. After filtration, the cartridge starts spinning again to release the sample towards the metering structure to let 20 µL through into the measuring chamber, in which the assay reagents are lyophilized. The signal is measured using diodes. Any excess volume will be collected in the waste compartment. After the measurement, the cartridge, including the reagents, can be discarded.

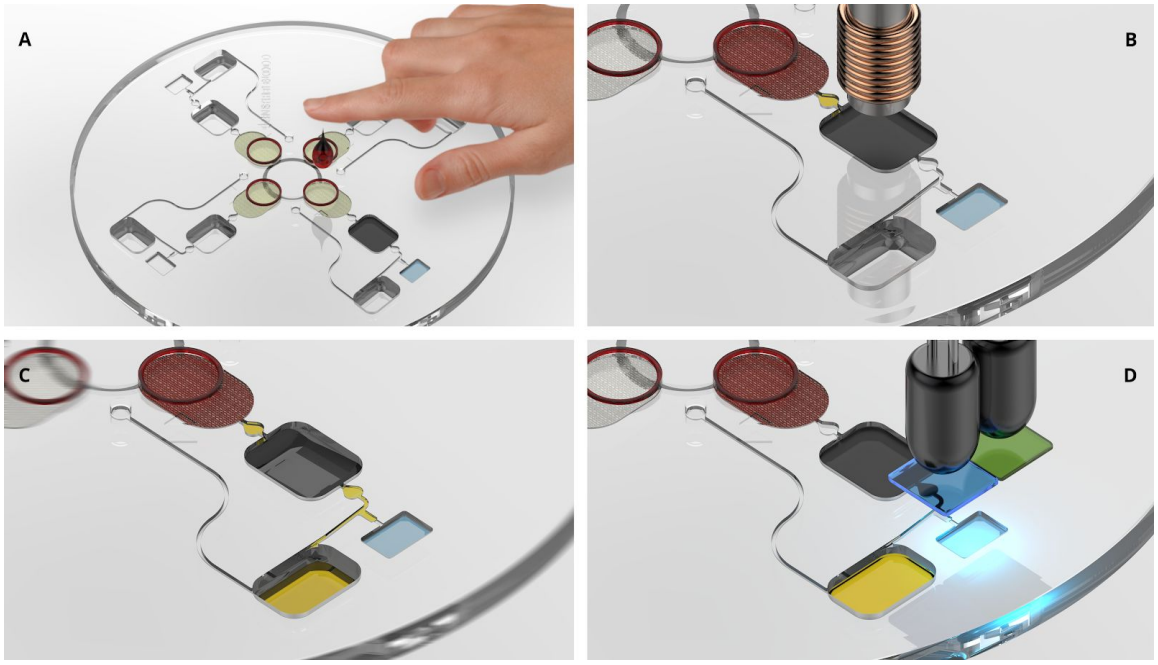

Fig. 1.2. *Cartridge Steps A) Place blood droplet at the inlet; B) Filter albumin from the blood plasma via magnetic separation; C) Measure the filtered sample volume for the assay ; D) Allow the assay to dissolve and measure the signal using diodes.*

1.3. Physical transduction

Two photodiodes (FD11A, Thorlabs) measure the light intensities from the assay- and reference signal. The diodes are positioned perpendicularly to the reaction chamber at a 2 mm distance (Fig. 1.2D). To separate the signals, a blue and a green dichroic filter (FD1B and FD1G, Thorlabs) are placed in front of the diodes. This ensures that two distinct signals are obtained from NanoBiT and mNeonGreen [11].

1.4. Reader instrument and user interaction

Fig. 1.3. *On the left, the mobile application; on the right, the biosensor included with the cartridge and lancing device*

The reader dimensions are 13.0 x 13.0 x 8.1 cm. Inside the device are the motor, electromagnets, diodes, cartridge holder, and a tiny computer. Appendix D includes a technical drawing of the interior of the device. The biosensor is operated by the epileptic patient (EP) through a mobile app. Every other day an EP can click on start measuring. The app instructs the user to prepare the lancing device, cartridge and reader. Then, the EP uses the lancing device to obtain a droplet of blood and lay their finger on the sample port. Inserting the cartridge starts the automated filtration and measuring process. After five minutes, the device sends the results to the phone via BlueTooth. Finally, the app requests the user to clean the lanced device and dispose of the cartridge. The app also reminds patients of their medicine intake. Throughout the day, people report any side effects in the app that is used to inform their doctor.

2. Technological Feasibility

To investigate the feasibility of the system, MATLAB was used to simulate the filtration and molecular recognition steps. In the first section, the filtration method is assessed based on filtering efficiency, time-to-result, and required reagent volume. The second section describes the relationship between the assay performance and initial reactants concentrations, concluding with an estimation for optimal initial conditions.

2.1 Filtration

Filtration via magnetic separation is considered feasible if the following two requirements are met. Firstly, we require that the bVPA concentration after filtration should be small compared to the fVPA concentration (typically less than 5%). Secondly, the fVPA concentration should remain the same before and after filtration. For the application of the proposed biosensor, the required conditions for magnetic separation should stay within the limits of the SensUs competition. This means that the reagent volume should be less than 200 µL and the time-to-result should remain within five minutes. In order to validate whether magnetic separation can be implemented, the filtration method was simulated. (See Appendix E1 for experimental methods).

2.1.1. Results

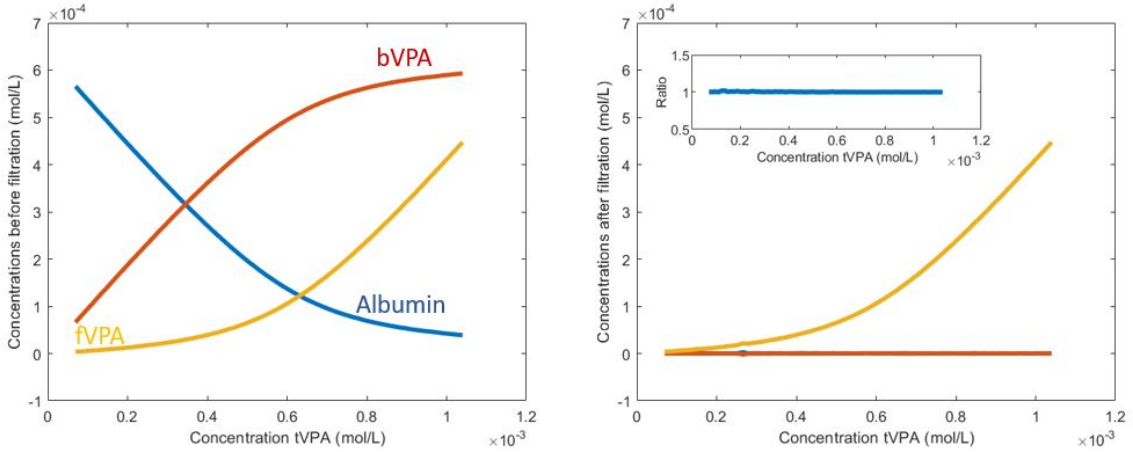

Fig. 2.1. Left) *The concentrations of fVPA, bVPA and albumin in mol/L before filtration.* ***Right)*** *The concentrations in mol/L after filtration with an anti-albumin antibody to albumin ratio of 18:1 (right). The inset shows the ratio between tVPA concentration after filtration and fVPA before filtration.*

The experiments were performed with a variation in antibody concentration. The resulting concentrations were measured after running the simulations for 30 seconds. Complete removal of albumin and bVPA is reached when the ratio between tVPA concentration after filtration and fVPA concentration before filtration is approximately one.

Fig. 2.1 shows the concentrations of fVPA, bVPA and albumin before and after filtration when a ratio of 18 mol antibody to 1 mol albumin is used during filtration. It can be seen that the concentration of fVPA before and after filtration remains the same and that albumin and bVPA are completely removed. This indicates that the filtration step does not influence the fVPA concentration. The inset shows that the ratio between tVPA after filtration and fVPA before filtration is approximately one, which is necessary for an accurate assay measurement.

2.1.2. Conclusion and discussion

The performance of magnetic separation is assessed based on time, filtering efficiency and volume. The filtration step is completed in 30 seconds, which is within the limit of the time-to-result of five minutes. The filtering efficiency is high considering complete albumin removal is reached when a ratio of 18:1 mol antibody to albumin is added to the system. However this translates to a volume of magnetic particles in solution of at least 140 mL for average albumin levels (Appendix E2). The volume of the magnetic particles solution needed for complete filtration exceeds the limits of the designed cartridge, thus this method cannot be used on its own for this application. Therefore, other separation options need to be explored to reduce the required volume. Potential filtration methods could be the combination of magnetic separation with another method which can be performed on a relatively small scale such as ultrafiltration membranes.

2.2 Assay

The bioluminescent immunoassay is considered feasible if the concentration coefficient of variation (CV) is lower than 10% over the whole range of fVPA (4-15 µg/mL). For the implementation of the assay in the proposed biosensor, the following requirements are determined. Firstly, the initial concentrations should be in the range of or below 1 µM. The assay must fit in the assay chamber, which has the size of 20 µL. Also, the signal intensity range should be detectable with the optical setup and the assay time-to-result should remain within 5 minutes. Simulations of the assay were performed to evaluate these criteria (See appendix F for experimental methods).

2.2.1. Results

To obtain insights about the influence of the initial VPA antibody and analogue concentrations on the dose-response curve (DRC), the simulations were performed for different values of VPA-Ab and VPAa while other conditions were kept constant. The NanoBit concentration after 10 seconds for a range of VPA concentration is plotted in Fig. 2.2. A shift in the ratio of VPAa and VPA on the antibody causes a shift in the DRC towards higher VPA concentrations for increasing VPAa concentrations (Fig. 2.2a). In the most linear and steepest part of the curve, the sensor is the most sensitive to VPA variations. There, the analog concentration matches the VPA concentration, because the competition between the two molecules is the strongest. Fig. 2.2b shows the variation in VPA antibody on the DRC. It appears that the antibody concentration has no effect on the DRC shape. However, the signal intensity scales with the order of antibody concentration caused by an increase in VPA-NB formation.

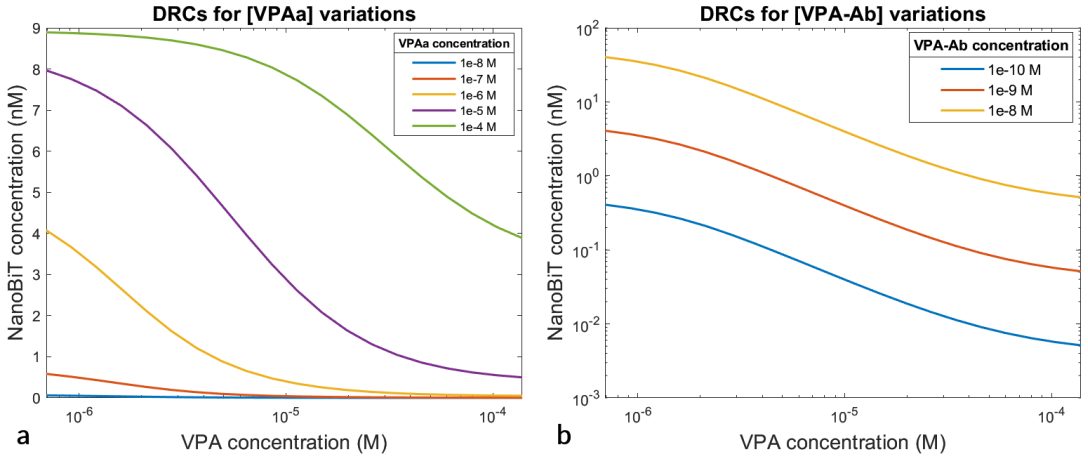

Fig. 2.2 *Dose-response curves in terms of NanoBit concentration according to variations of VPA-analog concentration (a) and VPA-antibody concentration (b).*

The VPA analogue and antibody concentrations in the biosensor are determined by the number of initial molecules that were lyophilized inside the cartridge and the volume of the assay chamber. Also, the time before measuring the signal and the dissociation constant between LargeBiT and SmallBiT affect the output of the assay [4]. For the aforementioned parameters the optimal initial conditions were calculated based on generated DRCs using the following predetermined conditions: dilution factor: 10x, assay volume: ~10 µL, furimazine concentration: 10 µM. Through the simulations the optimal initial conditions are found to be: VPA-Ab quantity: 10^{-13} mol, VPAa quantity: 10^{-11} mol, time before measuring: 10 seconds, NanoBiT dissociation constant: 10^{-4} M. The DRC resulting from this ideal case was calculated in terms of NanoBiT concentration for a wide VPA range (Fig. 2.3a). The CV for this DRC is determined using the intra-assay signal standard deviation of 6.57%. This value is estimated by T.E.S.T. 2019 from similar lab experiments. The calculated CV is less than 10% for the VPA concentration of 4-170µg/mL, which we define as the dynamic concentration range. Therefore, the range of this assay is sufficient for either fVPA or tVPA concentration measurements.

For the fVPA concentration range of 4-15 µg/mL, the furimazine and NanoBit concentration are used to calculate the photon count per second after 10 seconds, which is converted to a signal power that reaches the diode and the response electrical current (Fig. 2.3b).

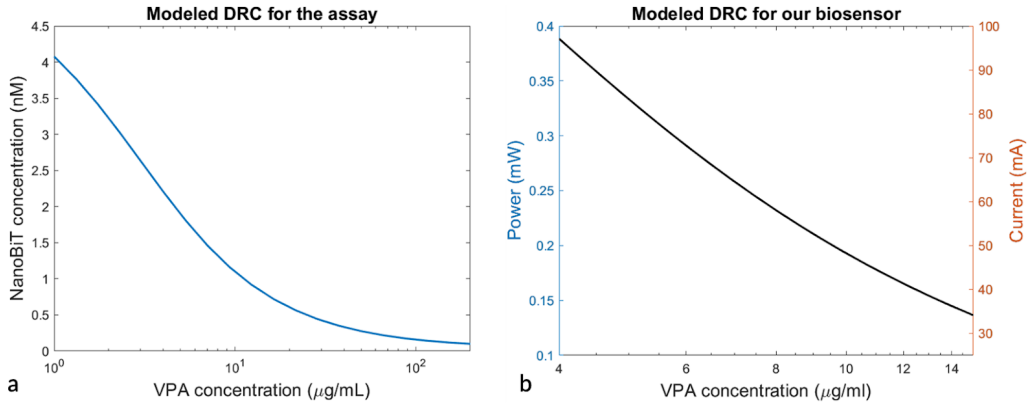

Fig. 2.3. (a) *The optimal dose-response curve in terms of NanoBit complex.* ***(b)*** *The dose-response curve for the fVPA concentration range in terms of power that reaches the diode (left-axis) and response current from the diode (right-axis).*

2.2.2. Conclusion and discussion

The optimal initial concentrations of VPA-Ab and VPAa correspond with an amount of material suitable for a sensor cartridge. The minimum current produced by the diodes is far above (10^{10} times) the dark current (SpecSheet FD11A, Thorlabs). Therefore, the signal intensity is detectable with the proposed optical setup. The assay time of 10 seconds complies with the general specification of a point-of-care device. The calculated CV below 10% implies a quantifiable fVPA concentration. To validate the performance of the assay in laboratory conditions, it is advised to start with the proposed optimal settings. The dynamic range of the assay can be adjusted by altering the analogue concentration. Furthermore, results indicate that increasing the antibody concentration raises the signal intensity.

However, some limitations should be noted. First, the model only takes into account the light emitted by NanoBit. In reality, LargeBiT on its own also produces a slight background signal [12]. Second, the model does not include the dissolution of the lyophilized assay reagents within plasma. This could take a considerable amount of time depending on the lyophilization technique and environmental conditions. Future experiments can show the influence of the dissolution on the assay time.

Nevertheless, we expect that the fVPA concentration can be quantified with the bioluminescent immunoassay and that the influence of the unknowns can be corrected for by performing empirical research in a laboratory setting.

3. Originality

3.1. Team

Assay principle. As a team, we envisioned a protein-based assay. First, we explored various methods, such as EMIT, ELISA, FPIA, and CEDIA. We consulted experts in the field of protein, chemical, industrial and biomedical engineering to make a concept decision. Then, together with prof. dr. M. Merkx, from the Department of Protein Engineering, we discussed the possibilities for a bioluminescent based sensor. We figured that this course would most leverage the expertise present within our university and knowledge from the previous team. Furthermore, it reduces the complexity of the detection method, which is favorable considering our team only has two electrical engineers.

Our team was responsible for the implementation of the concept. We, therefore, created models to find the optimal affinities of SmallBit and the antibodies. Furthermore, we investigated the protocols and papers for making the VPA analog. All in all, the assay concept is developed by combining (partially) existing concepts with the help of expertise and experience from outside the team. As a team, we then individually built, adjusted, and computationally tested this concept.

Cartridge. The centrifugal cartridge is inspired by the Skyla veterinary clinical chemistry analyzer. After the literature research, we concluded that a centrifugal device gives more options to control the fluidics. We adapted designs from literature to realize the steps needed for our biosensor.

Filtration. First, we focused on commercially available methods to separate VPA-albumin complexes and albumin from fVPA. Options included ultrafiltration, ultracentrifugation, and a depletion kit containing a resin. However, none of these methods met the five minute filtration time requirement. Then, our supervisor Leo van IJzendoorn suggested investigating magnetic separation. After initial literature research, we concluded that this method is promising to separate albumin from the sample. Therefore, we created simulations to investigate if the magnetic separation was a feasible filtration method, using the affinities between VPA and albumin and albumin and anti-albumin antibodies found in the literature. In conclusion, the filtration method was developed due to the suggestion of our supervisor but as a team, we investigated the promise and tested this concept in our simulation.

3.2. Supervisor

Assay principle. The team has performed independently a broad literature search for different assay principles that could detect fVPA in blood plasma. Inspired by the success of the team of last year they suggested that a competitive bioluminescent assay with a split-NanoLuc enzyme might be interesting to explore. They contacted professor M. Merkx at TU/e who is a known expert in this field in order to discuss the feasibility of several competitive assay principles that they developed by themselves based on existing literature. In a brainstorm session together with prof. Merkx, the suggestion of an analog coupled with a linker to the small-bit part of the bioluminescent NanoLuc enzyme was considered to be most promising. In addition it was planned to implement ratiometric measurements to enhance the assay stability, similar to the principle applied by the team of last year. The specific construct with the large-bit of the NanoLuc enzyme bound to the Fc part of the detection antibody was suggested by prof. Merkx who has experience with this approach.

Filtration. The separation of fVPA from tVPA has been explored considering many principles ranging from electrophoresis, applying spin-filters and washing with beads. Although the team concluded that a rigorous separation was not possible, they did perform original calculations on the efficiency of bead washing and decided to incorporate this principle in a cartridge design.

Assay performance simulations. After the lock-down, the team independently developed a model to combine the affinity-based assay kinetics with the enzyme kinetics to model the assay performance for a wide range of parameters. This was their own initiative. The supervisors did critically discuss the used methods and obtained results with the students, but they never helped with setting up the model calculations.

Cartridge design/sensor integration. The cartridge design is based on the spinning disc principle which is a known concept, but the team came up with an original design of the microfluidic circuit with integrated bead washing. The supervisors have not been involved and only asked critical questions.

3.3. Signatures

The undersigned declares that the originality statements of both the team and supervisors are true.

dr. ir. Leo van IJzendoorn

ir. Rafiq Lubken

Ernst Paul Swens

Jesse Jägers

4. Translation Potential

The translation potential is discussed in terms of the business model canvas, stakeholder desirability, and financial feasibility sections.

4.1. Business model canvas

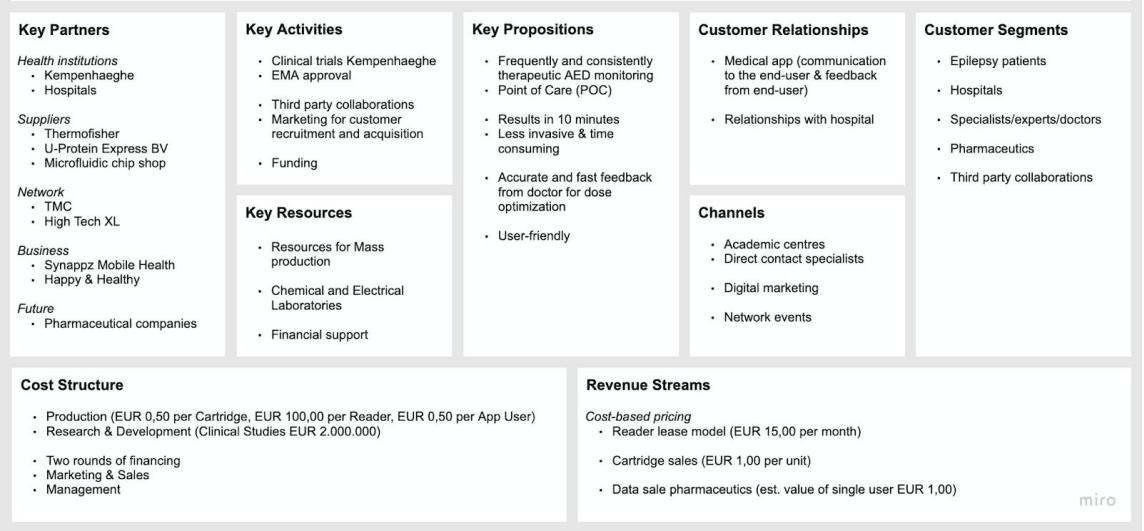

Fig. 4.1. *Business Model Canvas of T.E.S.T. 2020*

4.2. Stakeholder desirability

Around 1 in 150 people suffer from epilepsy worldwide, making it one of the most common neurological diseases [13]. Epilepsy affects approximately 120,000 people in the Netherlands [14]. Seven out of ten epileptic patients (EPs) generally live a seizure-free life, when properly diagnosed and treated [15]]. Prof. dr. H.J.M. Majoie and dr. R.H.C. Lazeron from the Academic Centre of Epilepsy, estimated that between 26% and 40% of EPs require therapeutic drug monitoring (TDM), due to doses that vary over time. This group includes especially pregnant women, elderly, and mentally disabled people [16][17][18].

4.2.1. State of art

To date, doctors determine the drug doses of EPs based on the patient's experiences. Unfortunately, there is no method to monitor patients frequently and consistently. A survey amongst patients (n=10), points out that EPs negatively experience hospital visits to measure anti-epileptic drugs (AEDs) in blood levels (Appendix H). The main reasons are invasive measuring, time-consuming, and receiving results takes 3-5 days. Besides the lowered quality of life of EPs, non-optimal dosing leads to an increase in spending for health care.

4.2.2. Value Proposition

The T.E.S.T. biosensor measures the concentration of AEDs within five minutes from home. A blood sample is obtained in a less invasive manner, using a lancing device. The patient will measure their blood concentration every other day and the app stores their data. Collecting not only AED levels but also seizures information, helps to improve the evaluation of the AED dosage. EPs can throughout the day report in the app frequency, duration, and side effects. Insurance companies mainly consider reimbursement of clinically proven and well-accepted therapies. Therefore, hospitals are considered our customers for the biosensor.

This approach is essentially a tool, not intended to replace professionals but to enable them to make better and faster decisions on AED dosage. Experts can send feedback to patients via the app to reduce routine appointments. Furthermore, the data-driven approach is of great value to pharmaceutical companies. For instance, UCB can develop new AEDs based on the feedback of patients' drug response [19]. The following five situations describe how patients will benefit from TDM in the treatment of epilepsy [20]:

1. determination of therapeutic concentration range,
2. aid in the diagnosis of clinical toxicity,
3. assessment of compliance in irregular and/or uncontrolled seizures,
4. guiding dosage adjustment in situation with pharmacokinetic variability,
5. anticipation of pharmacokinetic change.

4.3. Business feasibility

Fig. 4.2. *Overview of the stepwise approach, including the serviceable market, AEDs, and partners*

Studies conclude that the number of prescriptions of Levetiracetam (LEV) in Germany increased with 2681% between 2010 and 2017. In 2013, LEV became more prescribed than VPA. Moreover, the total expenditures of LEV is almost 2.5 times higher than VPA [21] [22] [23]. This information drives the decision to first focus on LEV and later extending our application to the second and third largest valued AEDs.

The business model consists of a stepwise approach (Fig. 4.2). In the first phase, the focus is solely on the Dutch market of LEV. In 2022, the serviceable available market broadens to the 4EU+UK (Germany, France, Italy, Spain, United Kingdom*). In the third phase, the product capabilities will extend from LEV monotherapy to polytherapy of LEV, VPA, and Lamotrigine (LTG).

4.3.1. Phase I Validation

The aim of phase one is to develop and validate the biosensor for LEV in collaboration with the Academic Centre of Epilepsy - Kempenhaeghe. Clinical trials will determine the effectiveness and safety of the biosensor. Before starting these clinical trials, our device must comply with the requirements of an in vitro diagnostic device class C (or IIb of the EMA) [24][25]. After approval, the reader and cartridges can start in small batch production. At this point, the technical team will consist of assay developers, microfluidics engineers, and electrical engineers, which aim to do production activities inhouse.

Alongside our team, more knowledge and experience about app development is required. Therefore, we seek to partner with *Synappz Mobile Health,* which is specialized in medical apps and located in the Netherlands. An online marketing campaign by *Happy&Healthy* intends to inform hospitals of our new innovative services. This company is specialized in healthcare marketing and located in Eindhoven. Besides online marketing, promotions take place via conferences. To find funding and increase our network we aim to partner up with *TMC* and *HightechXL*.

4.3.2. Phase II Growing

In 2022, we expand to the 4EU+UK market. The aim is to meet the EMA's IIb regulations and to reach half our serviceable obtainable market within two years. For sales, upscaling has to take place at a faster pace. Therefore, it is of great importance to outsource production. For instance, *U-Protein Express* can absorb protein expression and antibody production. Additionally, the German Microfluidic Chipshop can manufacture our CD-formatted cartridge.

4.3.3. Phase III Establishing

In 2024, our application scope extends to mono- and polytherapy of LEV, VPA, and LTG. These medications account for 31.4% of the prescribed AEDs [21]. The biosensor provides information that is essential for safe and effective use of an AED. Pharmaceutical companies, like *Desitin Arzneimittel GmbH*, can improve existing epileptic therapies with the use of our app data. Furthermore, data could help pharmacists to shorten the development time of new AED by gaining more qualitative knowledge from their target group. The biosensor remains close to the original design, though, each therapy requires a unique cartridge. To manage sales, we outsource production to larger companies, such as U-Protein Express BV and Thermo Fisher Scientific.

* During the transition period, any recommendations or decisions made by European Medicines Agency's scientific committees in the context of regulatory procedures of medicines will also apply in the UK [31]

4.4. Financial viability

In five years, the aim is to grow a startup focused on measuring LEV in the Netherlands to a multiplex platform in Europe. The startup phase involves the clinical development of the biomedical device. Studies will target a narrow target group of around 750 patients [25]. To interest hospitals in switching to our services, it is necessary to compete with the market prices of existing health care services. This value is around EUR 365.00 based on the average Dutch market price [26]. Initially, our strategy focuses on differentiation, whereas later stages are more cost-driven.

4.4.1. Market size

The serviceable available market (SAM) is estimated by multiplying the population size, people with epilepsy in the EU (82 per 100,000) and prescription of AEDs [21], [27] [28]. Prof. Dr. Marian Majoie, from the Academic Centre of Epilepsy considered the serviceable obtainable market (SOM) between 26% and 40% of the SAM. The Dutch SOM for LEV monotherapy is estimated around 8,200 (±21.2%) people. Entering the 4EU+UK expands the SOM to 153,000 (±21.2%). Finally, broadening the application to polytherapy of LEV, VPA, and LTG, in the 4EU+UK and the Netherlands increases the SOM to 290,000 (±21.2%). Market details are included in appendix A.

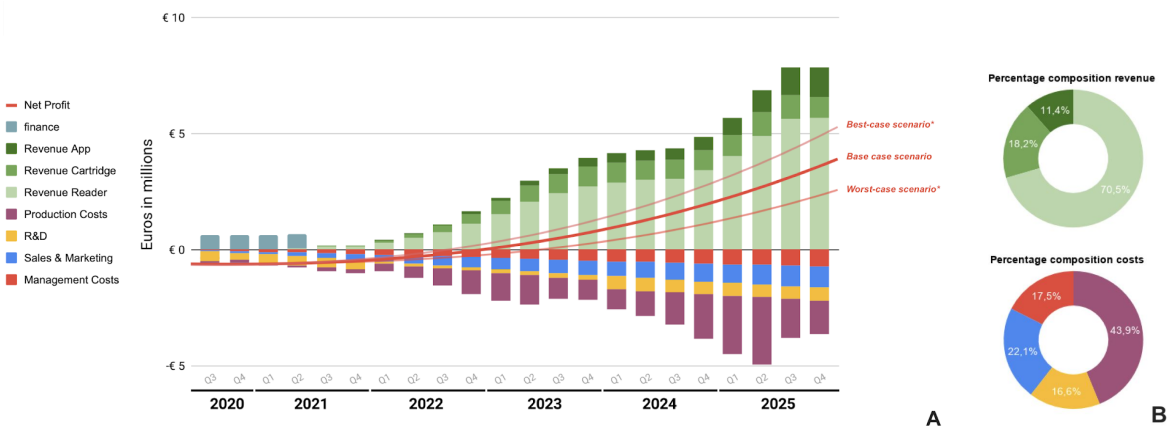

Fig. 4.3. *a) Five-Year Costs, Revenues and Profit Projection (** based on ±21.2% SOM differences) (b) Total Cost & Revenue percentages*

4.4.2. Cost structure

The costs structure consists of production, research & development, marketing & sales, and management costs. The unit production costs of a reader start at EUR 150 for small batch production down to EUR 100 for mass production. This prime cost is based on the bill of materials in appendix **C**. Similarly, the cartridge's prime costs range between EUR 2 down to EUR 0.50 [29]. The approximated R&D expenditure is founded on comparable clinical studies. For instance, the first clinical development is estimated at EUR 500,000 and EMA studies at EUR 1,500,000 [30] [31]. In total, T.E.S.T. requires EUR 2,500,000 in funding the first year.

4.4.3. Revenue structure

Revenue streams consist of the reader, cartridge, and app data. Hospitals lease the biosensor for EUR 20.00 per month. The leasing model reduces the entry costs for hospitals and decreases the reader's prime cost compared to a selling model. The cartridge unit selling price is EUR 1.00. The average duration of treatment is estimated at nine months using one cartridge every other day. Altogether, the therapy would cost EUR 315.00. The revenue from patient drug information to pharmaceutical companies is EUR 1.00 per user. More information on the cost and revenue structure of the company is available in the appendix B.

4.4.4. Financial Projection

Fig. 4.3. shows the five-year financial projection. In the first year, hospitals will lease 354 readers and purchase 47,800 cartridges. This period yields a loss of EUR 2,200,000. In the second half of 2022, the expansion to 4EU+UK starts, allowing us to sell in larger volumes. In the period between late 2022 and early 2023, the company will reach the break-even point, totaling EUR 3,810,000 of profit. After a period of 5 years, hospitals leased 94,400 biosensors and purchased almost 14 million cartridges. Averaging an operating profit margin of 23,2% and margin on sales of 66,3%.

At this point, T.E.S.T. has accomplished its mission to become a mid-sized biotech company well established in the European market. This concludes the translation potential of our business.

5. Team and Support

The multidisciplinary T.E.S.T. 2020 team consists of ten students from the Chemical, Biomedical, and Electrical Engineering Departments, including both Bachelor and Master students. In the first three months, all team members focused on literary research. Starting from February 2020, we divided responsibilities among team members. Due to COVID-19, the TU/e prohibited lab access to student teams. This new situation required role and responsibility adjustments among the team members.

5.1. Contributions of the Team Members

We will start by introducing our chairman, **Ernst Paul Swens**, who has been managing the team and made sure the project and collaboration ran smoothly. Besides his leadership task, he has also been working on the reader and has helped the Translation Potential (TP) sub-team during COVD-19 as reinforcement.

Jesse Jägers has been vice-chair of the team and was initially involved with assay development and business case. During COVID-19, Jesse has proven himself to be helpful in every sub-team that needed reinforcement and has led the team together with Ernst Paul.

Our Treasurer, **Eveline Nugraha**, has kept track of all the finances and helped with assay development. During COVID-19, she was the main contributor to the assay simulations in Matlab.

Maurits van der Vorm has been a member of the filtration sub-team and active with the business case. During COVID-19, he has focused on TP and greatly contributed to the end-result of this team.

Thomas Stekelenburg initially worked on the reader and its design, but during COVID-19 supported with MATLAB simulations.

Leandra Vermeulen has initially been a member of the Assay sub team because she has great lab experience, but during COVID-19 she was mainly working on cartridge design and development.

The Filtration team was led by **Caitlin Pieneman.** She has continued working in this team during COVID-19 and was the main contributor to the filtration simulation in MATLAB.

Melle Houben has been a member of the Filtration sub team and was also contributing to the TP sub team. During COVID-19 he left the Filtration sub team to focus on the business case in the TP sub team.

Our head of Public and External Relations, **Imke Rodenburg**, was initially a member of the Assay sub team. During COVID-19, she switched to the TP sub team because reinforcement was necessary.

Mirre Trines has been a member of the Assay sub team and was next to Imke a member of the Public and External Relations team. During COVID-19, it was also necessary for her to switch to the TP sub team.

5.2. People who have given support

The main support was given by our supervisors **Leo van IJzendoorn** and **Rafiq Lubken**. They have been giving advice to the entire team throughout the whole year. They managed to direct the team into the right way but gave us a lot of freedom to discover the different paths ourselves at the same time. Both have expertise in useful research fields so they could provide advice to all sub teams. Before COVID-19, **Claudia Schot** was also present during our weekly meetings, but her importance decreased during COVID-19 because lab access was prohibited. **Maarten Merkx** has provided us with crucial information and advice for the biochemical assay. **Marian Majoie**, a neurologist at Kempenhaeghe, has provided us with useful insights in AEDs and epilepsy that contributed to the business case. Employees of **HighTechXL** and **Future Diagnostics** have supported us by providing advice and information on both assay, filtration design, and the business case.

5.3. Sponsors

In this section we explicitly want to thank the **Studenten Fonds TU/e** for providing us financial support to realize this project.

6. Final Remarks

It has been a great experience to work on this project together even under the unexpected circumstances of 2020.

In the future, some of us might continue to work on similar topics during internships. We think that our models could be improved using data from lab experiments such as the light intensity that is produced and the maximum output that can be measured by the diodes with optionally an additional amplifier.

We like to end on a note of appreciation. Thank you to everyone who has supported us in our journey. Especially Leo, Rafiq and Claudia, we could not have done this without your guidance.

References

1. I. Safarik and M. Safarikova, “Magnetic techniques for the isolation and purification of proteins and peptides,” *BioMagnetic Research and Technology,* vol. 2, no. 7, 2004.

2. X. Yang, J. Janatova, J. M. Juenke, G. A. McMillin and J. D. Andrade, “An ImmunoChip prototype for simultaneous detection of antiepileptic drugs using an enhanced one-step homogeneous immunoassay,” *Analytical Biochemistry,* vol. 365, no. 2, pp. 222-229, 2007.

3. M. P. Hall, J. Unch, B. F. Binkowski, M. P. Valley, B. L. Butler, M. G. Wood, P. Otto, K. Zimmerman, G. Vidugiris, T. Machleidt, M. B. Robers, H. A. Benink, C. T. Eggers, M. R. Slater, P. L. Meisenheimer, F. Fan, D. H. Klaubert, L. P. Encell and K. V. Wood, "Engineered luciferase reporter from a deep sea shrimp utilizing a novel imidazopyrazinone substrate," *ACS Chem Biol,* vol. 7, no. 11, pp. 1848-1857, 2012.

4. A. S. Dixon, M. K. Schwinn, M. P. Hall, K. Zimmerman, P. Otto, T. H. Lubben, B. L. Butler, B. F. Binkowski, T. Machleidt, T. A. Kirkland, M. G. Wood, C. T. Eggers, L. P. Encell en K. V. Wood, „NanoLuc Complementation Reporter Optimized for Accurate Measurement of Protein Interactions in Cells,” *ACS Chemical Biology ,* vol. 11, nr. 2, pp. 400-408, 2016.

5. J. Z. Hui, S. Tamsen, Y. Song en A. Tsourkas, „LASIC: Light Activated Site-Specific Conjugation of Native IgGs,” *Bioconjugate Chemistry,* vol. 26, nr. 8, pp. 1456-1460, 2015.

6. C. G. England, E. B. Ehlerding en W. Cai, „NanoLuc: A Small Luciferase Is Brightening Up the Field of Bioluminescence,” *Bioconjugate Chemistry,* vol. 27, nr. 5, pp. 1175-1187, 2016.

7. D. Mark, T. Metz, S. Haeberle, S. Lutz, J. Ducree, R. Zengerleab en F. von Stetten, „Centrifugo-pneumatic valve for metering of highly wetting liquids on centrifugal microfluidic platforms,” *Lab on a Chip,* vol. 9, pp. 3599-3603, 2009.

8. M. Focke, F. Stumpf, B. Faltin, P. Reith, D. Bamarni, S. Wadle, C. Müller, H. Reinecke, J. Schrenzel, P. Francois, D. Mark, G. Roth, R. Zengerle en F. v. Stetten, „Microstructuring of polymer films for sensitive genotyping by real-time CPR on a centrifugal microfluidic platform,” *Lab on a Chip,* vol. 10, pp. 2519-2526, 2010.

9. J. M. Cheng, P.-C. Huang en M.-G. Lin, „Analysis and experiment of capillary valves for microfluidics on a rotating disk,” *Microfluidics and Nanofluidics,* vol. 4, pp. 427-437, 2008.

10. S. Hin, M. Loskyll, V. Klein, M. Keller, O. Strohmeier, F. von Stetten, R. Zengerle en K. Mitsakakis, „Membrane-based sample inlet for centrifugal microfluidic cartridges,” *Microelectronic Engineering,* Vols. %1 van %2187-188, pp. 78-83, 2017.

11. E. J. Aird, K. J. Tompkins, M. P. Ramirez en W. R. Gordon, „Enhanced Molecular Tension Sensor Based on Bioluminescence Resonance Energy Transfer (BRET),” *ACS Sensors,* vol. 5, nr. 1, pp. 34-39, 2020.

12. Promega NanoBiT® Protein:Protein Interaction System Technical Manual, Chapter 7.A. Relative Luminescence of Specific versus Nonspecific Interactions.

13. WHO, "Epilepsy: a public health imperative," World Health Organization, 2019.

14. Epilepsiefonds, "Bij wie en op welke leeftijd," 2020. [Online]. Available: https://www.epilepsie.nl/over-epilepsie/pagina/224-1/bij-wie-en-op-welke-leeftijd/.

15. M. J. Eadie, "Shortcomings in the current treatment of epilepsy," Expert Review of Neurotherapeutics , pp. 1419-1427, 2014.

16. S. C. Schachter, J. I. Sirven and K. J. Meador, "Risks During Pregnancy," 7 March 2014. [Online]. Available: https://www.epilepsy.com/living-epilepsy/women/epilepsy-and-pregnancy/risks-during-pregnancy.

17. C. W. McGrother, S. Bhaumik, C. F. Thorp, A. Hauck, D. Branford and J. M. Watson, "Epilepsy in adults with intellectual disabilities: Prevalence, associations and service implications," Seizure, vol. 15, no. 6, pp. 376-386, 2006.

18. S. K. Lee, "Epilepsy in the Elderly: Treatment and Consideration of Comorbid Diseases," Epilepsy Research, vol. 9, no. 1, pp. 27-35, 2019.

19. UCB, "A global biopharma company, focusing on neurology and immunology," UCB, 20 February 2020. [Online]. Available: https://www.ucb.com/our-company/.

20. P. Patsalos, D. Berry, B. Bourgeois, J. Cloyd, T. Glauser, S. Johannessen, I. Leppik, T. Tomson and E. Perucca, "Antiepileptic drugs—best practice guidelines for therapeutic drug monitoring: A position paper by the subcommission on therapeutic drug monitoring, ILAE Commission on Therapeutic Strategies.," Epilepsia, vol. 49, pp. 1239-1276, 2008.

21. N. Vyas, S. Shahani and M. Gandhi, "Prescription pattern of antiepileptic drugs in seizure disorder, their adverse reactions and cost analysis: A tertiary care hospital-based study," National Journal of Physiology, Pharmacy and Pharmacology, vol. 10, no. 3, pp. 215-220, 2020.

22. L. M. Willems, H. M. Hamer, S. Knake, F. Rosenow, J. P. Reese and A. Strzelczyk, "General Trends in Prices and Prescription Patterns of Anticonvulsants in Germany between 2000 and 2017: Analysis of National and Cohort-Based Data.," Applied health economics and health policy, vol. 17, no. 5, pp. 707-722, 2019.

23. Zorginstituut Nederland, "Aantal gebruikers 2015-2019 voor ATC-subgroep N03A : Anti-epileptica," GIP, 2020.

24. Global Harmonization Task Force, "Principles of in vitro diagnostic (IVD) medical devices classification," 2007.

25. EU, "REGULATION (EU) 2017/745 OF THE EUROPEAN PARLIAMENT AND OF THE COUNCIL," Official Journal European Union, 2020.

26. Nederlandse Zorgautoriteit, "Open data van de Nederlandse Zorgautoriteit," Nederlandse Zorgautoriteit, 2019. [Online]. Available: https://www.opendisdata.nl.

27. WHO, "European region: fostering epilepsy care in Europe," Epilepsia, 2011.

28. Eurostat, "Population and population change statistics," August 2020. [Online]. Available: https://ec.europa.eu/eurostat/statistics-explained/index.php/Population_and_population_change_statistics#EU-27_population_continues_to_grow.

29. Microfluidic ChipShop, "Lab-on-a-Chip Catalogue," 2011.

30. EMA, "Questions & Answers on Implementation of the Medical Devices and In Vitro Diagnostic Medical Devices Regulations ((EU) 2017/745 and (EU) 2017/746)," Human Medicines Evaluation Division, 2019.

31. EMA, "Fees payable to the European Medicines Agency," 2020. [Online]. Available: https://www.ema.europa.eu/en/human-regulatory/overview/fees-payable-european-medicines-agency.

32. Y. Kodama, Y. Koike, H. Kimoto, F. Yasunaga, M. Takeyama, I. Teraoka en I. Fujii, „Binding parameters of valproic acid to serum protein in healthy adults at steady state," *Therapeutix drug monitoring,* vol. 14, nr. 1, pp. 55-60, 1992.

Appendices

The appendices provide more detailed information about:

- Appendix A Market Size
- Appendix B Financial Projection
- Appendix C Bill of Materials Reader
- Appendix D Technical Drawing Reader
- Appendix E1 Filtration feasibility: Experimental Methods
- Appendix E2 Filtration feasibility: Calculation volume of magnetic particles
- Appendix F Assay Feasibility Experimental Methods
- Appendix H Survey Kempenhaeghe

Appendix A Market Size Details

Table A.1. *Different markets estimated for EPs and AEDs prescription in 4EU + UK*

Population	Total addressable market (TAM) *1	Serviceable available market (SAM) *2		Serviceable obtainable market (SOM) *3	
		Levetiracetam (Monotherapy)	*VPA, LEV, LTG (Polytherapy)*	*Levetiracetam (Monotherapy) min - max*	*VPA, LEV, LTG (Polytherapy) min - max*
The Netherlands	**141,696**	**24,797**	**44,493**	**6,448 - 9,918**	**11,567 - 17,798**
5 EU	**279,8168**	**464,883**	**878,625**	**120,870 - 185,954**	**228,443 - 351,450**
France	*549,318*	*96,131*	*172,486*	*24,995 - 38,453*	*44,847 - 68,995*
Great Britain	*546,530*	*95,643*	*171,610*	*24,868 - 38,258*	*44,619 - 68,644*
Germany	*680,764*	*119,134*	*213,760*	*30,975 - 47,654*	*55,578 - 85,504*
Italy	*494,952*	*86,617*	*155,415*	*22,521 - 34,647*	*40,408 - 62,166*
Spain	*384,908*	*67,359*	*120,861*	*17,514 - 26,944*	*31,424 - 48,345*

*1 $Population\ size * EU\ average\ epilepsy\ (82\ per\ 100,000)$

*2 $TAM * \%\ AEDs\ (LEV\ monotherapy,\ 0,175;\ VPA,\ LEV,\ LTG\ (Polytherapy),\ 0,314)$

*3 $SAM * [24-40]\%$ (*estimated based on Prof. Dr. Marian Majoie, from the Academic Centre of Epilepsy*)

Appendix B Financial Projection Details

Table B.1. *Detailed Yearly Financial Projection*

Year	2020	2021	2022	2023	2024	2025
Revenue	**€ 27.125**	**€ 431.430**	**€ 3.845.215**	**€ 12.657.481**	**€ 17.584.878**	**€ 28.206.976**
Reader *1	€ 18.115	€ 291.034	€ 2.625.266	€ 8.754.484	€ 12.348.385	€ 20.174.336
Cartridges *2	€ 8.917	€ 130.152	€ 1.034.580	€ 2.954.508	€ 3.361.092	€ 3.923.583
App *3	€ 93	€ 10.243	€ 185.369	€ 948.490	€ 1.875.401	€ 4.109.057
Costs	**€ 853.834**	**€ 3.392.295**	**€ 5.921.239**	**€ 8.847.538**	**€ 12.545.134**	**€ 16.932.548**
Production *4	€ 68.368	€ 431.581	€ 2.565.446	€ 4.232.639	€ 5.289.898	€ 8.554.482
R&D *5	€ 577.036	€ 1.697.449	€ 550.850	€ 762.304	€ 2.186.122	€ 2.216.722
Marketing & Sales *6	€ 108.977	€ 698.299	€ 1.402.471	€ 2.145.345	€ 2.829.795	€ 3.452.100
Management *6	€ 99.453	€ 564.966	€ 1.402.471	€ 1.707.250	€ 2.239.319	€ 2.709.243
Profit	**-€ 826.708**	**-€ 2.960.865**	**-€ 2.076.024**	**€ 3.809.943**	**€ 5.039.743**	**€ 11.274.429**
Operational Profit Margin *7	-3047,73%	-686,29%	-53.99%	30.10%	28.66%	39.97%
Selling Margin *8	-152,04%	-0,04%	33.28%	66.56%	69.92%	69.67%
# EPs *9	101	1702	16130	56540	84230	146322
# Readers *10	101	1,352	10,515	9,923	19,168	53,345
Price	€ 149	€ 142	€ 132	€ 123	€ 113	€ 104
# Cartridges ($\times 10^3$) *11	14	230	2177	6785	8844	13169
Price	€ 2.00	€ 1.70	€ 1.40	€ 1.10	€ 0.80	€ 0.50
# Employees *12	10	15	30	40	45	50

*1 *#Reader * Monthly Leasing Price * Average duration of treatment* (9 *months*)
*2 *#Cartridges * Cartridge Price*
*3 *#EPs * Data value per User*
*4 *#Reader * Prime cost Reader + #Cartridges * Prime cost Cartridges + #EPs * Prime cost App +#Employees * Percentage Production* (30%)
*5 *Clinical Development + EMA studies + #Employees * Percentage R&D* (30%)
*6 *Estimated between* 20 − 40% *of total costs*
*7 (*Revenue − Total Costs*)/*Revenue*
*8 (*Revenue − Production Costs*)/*Revenue*
*9 (*SOM Phase* 1 (24796) + *SOM Phase* 2 (460211) + 0.5 * *SOM Phase* 3 (878625)) * [24 − 40]%
*10 $max(quartile_n - sum(quartile_{n-3} : quartile_1), 0)$ * 90% (*percentage readers usable after leasing period*)
*11 *#EPs * Average duration of treatment* (9 *months*) * *Cartridges per Month* (15)
*12 *Estimated at similar sized companies, such as BioLogic Science Instruments and PalmSens BV*

Appendix C Bill of Materials Reader

Table C.1. Bill of Materials Reader

Name	Description	Quantity	Price	Distributor
Housing	Injection moulded part	1	*€ 5,00*	**1*
Computer	Orange Pi Zero with BlueTooth	1	*€ 5,00*	Allibaba
Electromagnet	Controllable magnets for the filtration step	*8*	*€ 3,00*	Allibaba
Diode *PL450B*	Diodes to measure signal and reference	*2*	*€ 34,16*	Thor Labs
Visible Bandpass Filter *480nm FWHM 25nm*	Filter placed in front of the diodes	*2*	*€ 11,53*	Optical Filtershop
Motor *RC300*	Motor for spinning the cartridge	*1*	*€ 9,95*	RS Components
Motor *24BYJ48*	Motor injecting and ejecting the cartridge	*2*	*€ 1,95*	RS Components
Cartridge Holder	Injection moulded part	*1*	*€ 5,00*	**1*
Accessoires *e.g. screws, cables ...*		-	*€ 5,00*	**2*
Total			***€ 149,23***	

*1 *Estimation based on prices of injection moulding process*

*2 *Estimation based on prices of standardized parts*

Appendix D Technical Drawing Reader

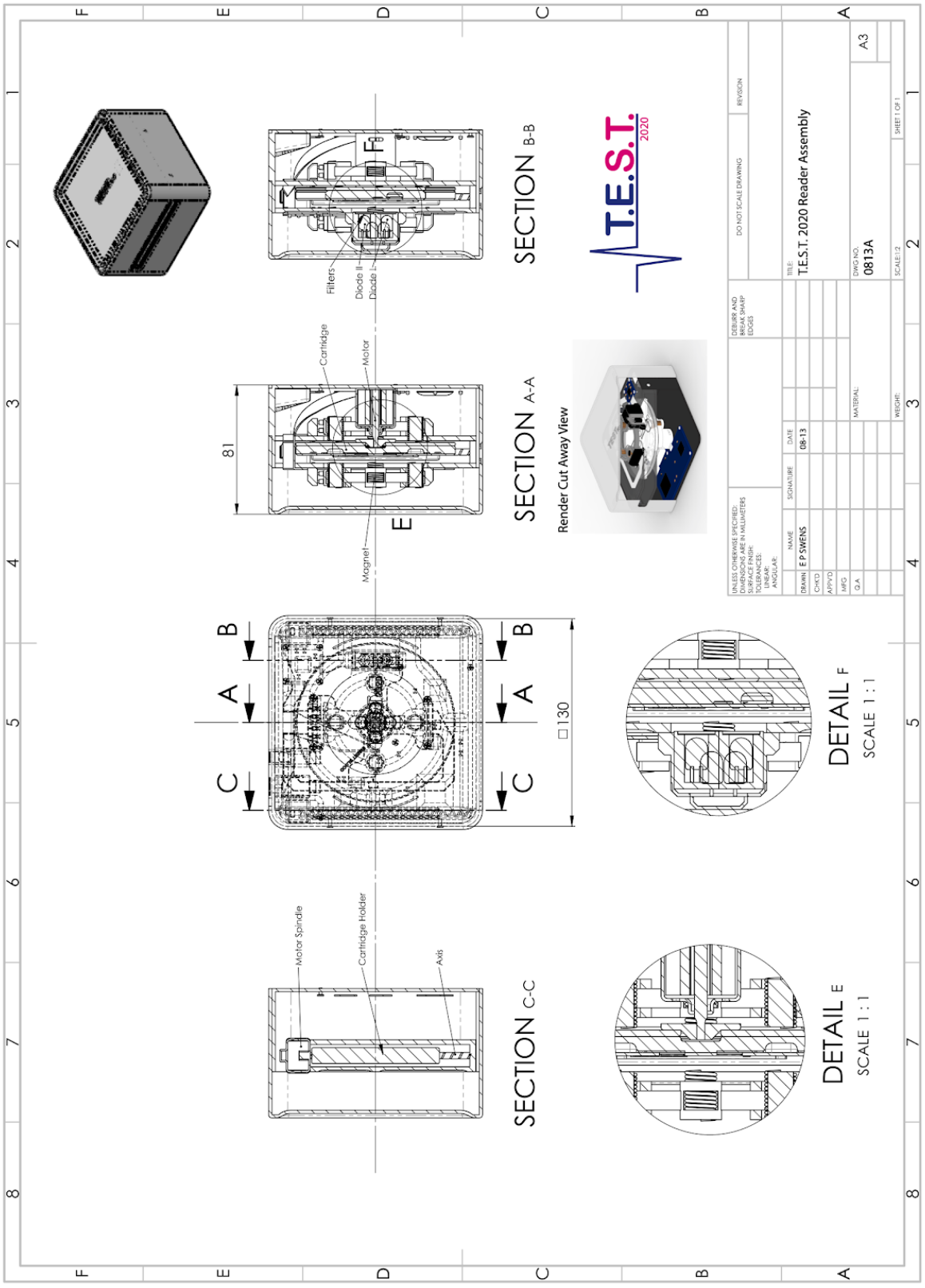

Fig. D.1. Technical Drawing of the Reader

Appendix E1 Filtration feasibility: Experimental Methods

The filtration method was simulated in three consecutive steps, as shown in Fig. E1. The concentrations of the components in equilibrium were determined before, during and after the filtration.

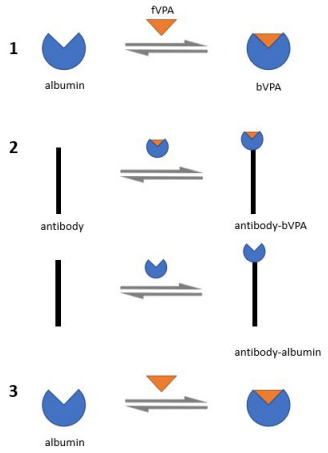

Fig. E.1. *The three-steps filtration method simulation*

In the first step, the concentrations of albumin, bVPA and fVPA in the sample in equilibrium were determined. This was done using the mean albumin level of 42 g/L and the range of total VPA of 10-150 µg/mL. For the formation of complex bVPA, a dissociation constant (Kd) of $3.67*10^{-5}$ M and an association rate (kon) of 10^5 $M^{-1}s^{-1}$ were assumed. Furthermore, the mean number of available binding sites per albumin molecule for VPA was estimated to be 1.26. [32]
In the second step, the magnetic particles are added to the system. The anti-albumin antibodies on the magnetic particles interact with both albumin and bVPA. Based on the assumption that the binding affinity between the antibody and albumin or antibody and bVPA are equal, the formation of both complexes were modelled with an assumed Kd of 10^{-8} M and kon of 10^5 $M^{-1}s^{-1}$.
When the equilibrium in the second step is reached, the magnetic particles are isolated. The solution then includes fVPA and the potentially remaining albumin and bVPA. In the last step, the final equilibrium between fVPA and the remaining albumin and bVPA were determined using the same parameters as step one.

Scripts

```
%Initial Conditions
n          = 1.26;                 % Number of binding sites obtainable
V_M        = 144.211;              % Molar mass valproate (g/mol)
Al_M       = 66500;                % Molar mass albumin (g/mol)

K          = 1/(2.72*10^4);        % Dissociation constant albumin-VPA complex (M)
kon        = 10^5;
koff       = K*kon;

K_2        = 10^-8;                % Dissociation constant albumin-antibody (M)
kon_2      = 10^5;
koff_2     = K_2*kon_2;

Al0_gl     = 42;                   % Average albumin concentration (g/L)
Al0        = Al0_gl/Al_M;          % Average albumin concentration (mol/L)
V0_gL      = linspace(.010,.15,75); % Conc tVPA 10-150 (ug/ml)
V0         = V0_gL/(V_M);          % Conc tVPA (mol/L)

%Creating Design of Experiments
DOF = fullfact([size(Al0,2) size(V0,2)]);
DOF = [(Al0*ones(size(DOF,1),1)) V0(DOF(:,2))'];
```

```
DOF = [DOF zeros(3,size(DOF,1))'];
f1 = @(t,x) Filtration_ODE(t,x,[kon,koff,n]);
f2 = @(t,x) Filtration_ODE_2(t,x,[kon_2,koff_2]);
f3 = @(t,x) Filtration_ODE_3(t,x,[kon,koff,n]);

%Running Experiments step I
for i = 1:size(DOF,1)
   [t,x] = ode45(f1,[0 10], [DOF(i,1) DOF(i,2) 0]);
   DOF(i,3) = x(end,1);                % Concentration albumin (mol/L)
   DOF(i,4) = x(end,2);                % Concentration fVPA (mol/L)
   DOF(i,5) = x(end,3);                % Concentration bVPA (mol/L)
end

%Running Experiments step II
for i = 1:size(DOF,1)
   [t,x] = ode45(f2,[0 30], [DOF(i,3) DOF(i,5) (18*DOF(i,3)) 0 0]);
   DOF(i,6) = x(end,1);                % Concentration albumin (mol/L)
   DOF(i,7) = x(end,2);                % Concentration bVPA (mol/L)
   DOF(i,8) = x(end,3);                % Concentration anti-albumin antibodies (mol/L)
   DOF(i,9) = x(end,4);                % Concentration antibody-albumin complex (mol/L)
   DOF(i,10) = x(end,5);               % Concentration antibody-bVPA complex (mol/L)
end

%Running Experiments III
for i = 1:size(DOF,1)
   [t,x] = ode45(f1,[0 10], [DOF(i,6) DOF(i,4) DOF(i,7)]);
   DOF(i,11) = x(end,1);               % Concentration albumin (mol/L)
   DOF(i,12) = x(end,2);               % Concenration fVPA (mol/L)
   DOF(i,13) = x(end,3);               % Concentration bVPA (mol/L)
end

%Systems of Equations I
function f = Filtration_ODE(~,x,p)
   %State variables
   Al   = x(1);
   V    = x(2);
   AlnV = x(3);

   kon = p(1);
   koff = p(2);
   n = p(3);

   %ODEs
   f(1)  =  koff * AlnV - kon*Al*V*n;          % dAl
   f(2)  =  koff * AlnV - kon*Al*V*n;                  % dfVPA
   f(3)  =  kon * Al*V*n - koff*AlnV;          % dbVPA

   f = f(:);
end

%Systems of Equations II
function f = Filtration_ODE_2(~,x,p)
   %State variables
   Al   = x(1);
   AlnV = x(2);
   Ab   = x(3);
   AlAb = x(4);
   AlnVAb = x(5);

   kon_2  = p(1);
   koff_2 = p(2);
```

```
   %ODEs
   f(1) = koff_2*AlAb - kon_2*Ab*Al;                                   %dAl
   f(2) = koff_2*AlnVAb - kon_2*Ab*AlnV;                               %dbVPA
   f(3) = koff_2*AlAb - kon_2*Ab*Al + koff_2*AlnVAb - kon_2*Ab*AlnV;   %dAb
   f(4) = kon_2*Ab*Al - koff_2*AlAb;                                   %dAb-Al
   f(5) = kon_2*Ab*AlnV - koff_2* AlnVAb;                              %dAb-bVPA

   f = f(:);
end
```

7. Systems of Equations III

```
function f = Filtration_ODE_3(~,x,p)
   %State variables
   Al   = x(1);
   V    = x(2);
   AlnV = x(3);

   kon = p(1);
   koff = p(2);
   n = p(3);

   %ODEs
   f(1)  =  koff * AlnV - kon*Al*V*n;          % dAl
   f(2)  =  koff * AlnV - kon*Al*V*n;                  % dfVPA
   f(3)  =  kon * Al*V*n - koff*AlnV;          % dbVPA

   f = f(:);
end
```

Appendix E2 Filtration feasibility: Calculation volume of magnetic particles

Binding capacity magnetic particles (MP): ~8 µg of human IgG per mg of beads
Dynabeads™ Protein G contains 30 mg/mL of beads in phosphate buffered saline
$M_{antibody}$ ~ 150 kDa = 150000 g/mol
Binding capacity MB = (8 μg)/(150000 g/mol)= $5.33*10^{-11}$ ($mol\ IgG$)/($mg\ MB$)
$c_{albumin} = 6.32*10^{-4}$ mol/L
$n_{albumin} = 6.32*10^{-4} * 20*10^{-6} = 1.26*10^{-8}$ mol
$n_{antibody} = 18* 1.26*10^{-8} = 2.27*10^{-7}$ mol
$m_{MP} = 2.27*10^{-7}/5.33*10^{-11} = 4255$ mg MP
$V_{MP} = 4255/30 = 141$ mL

Appendix F Assay Feasibility Experimental Methods

The biosensing kinetics were simulated starting with three initial components: VPA-Ab, VPAa and fVPA. Complexes were formed between VPA-Ab and VPAa or VPA through antibody paratope binding. For the formation of both complexes, an on-rate of 10^5 $M^{-1}s^{-1}$ and an off-rate of 10^{-3} s^{-1} were assumed. The enzyme NanoBiT was formed by the binding of SmallBiT, as a part of the VPAa molecule, and LargeBiT, as a part of the VPA-Ab molecule. The behavior was simulated of the three initial components to form a set of six different possible complex combinations (Fig. F1), out of which 4 complexes contained a complete NanoBiT complex that is bioluminescent. 3 of the these complexes are nonspecific to the VPA concentration, while only one complex gives the assay-specific signal. Dose-response curves were produced by running the simulations for 10 seconds on a range of initial VPA concentrations and summing the concentrations of the four bioluminescent complexes at the last time point.
The NanoBiT complexes that can be bioluminescent undergo an enzyme reaction with the substrate furimazine, in which the NanoBiT complex acts as an enzyme. The reaction causes furimazine to be converted to high energy furimadide. This high energy furimadide will fall back into a lower energy state during which it emits a photon. This means that the products of the enzyme reaction are: a photon, furimadide and the unchanged NanoBiT complex. This reaction was modeled with Michaelis-Menten kinetics.

To find the optimum combination of starting conditions, limitations on the enzyme kinetics were considered. The enzyme kinetics simulations showed that for an initial furimazine concentration of 10µM, the NanoBiT concentration for a signal that remains stable for longer than 10 seconds, needs to be lower than 10nM.
Based on an assay volume in the order of 10µL, dilution factor of 10 and a median signal lower than 10nM, the most optimal starting conditions were calculated as follows: The simulations were run for different values of these parameters for a range of 4 - 15 µg/mL VPA. The outcome was graded according to a Grey relational analysis in which an optimum dose-response curve was defined to have a high log-linearity, high median signal, wide signal intensity range, and a low fraction of nonspecific over specific signaling complexes.

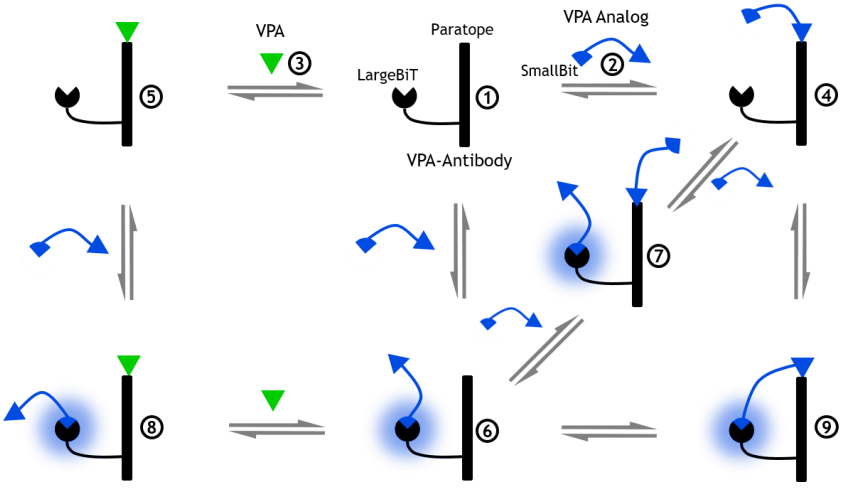

Fig. F.1. *With the assay simulations, out of 3 initial molecules, 6 complex combinations can be formed which were all modeled. Complex 6, 7 and 8 resemble nonspecific signaling complexes and complex 9 is the specific signaling complex.*

Scripts

Assay

```
function [pos_NL, neg_NL] = VPA_Assay(Vbounds,Am0,Cm0,v_as,DF,tspan,K)
%Inital conditions
%V0 = [lower bound, upper bound] (ug/mL)
%Am0 = 10^-7;                  %Initial antibody amount in mol
%Cm0 = 10^-4;                  %Initial VPA conjugate amount in mol
%v_as : volume of assay chamber
%v_fil : volume of filtration reagents
%tspan :    time span over which to do the differential equations
%K_values : KonV, KdV, KonC, KdC, konNL, KdNL
%pos_NL : concentration of specific signaling complexes
%neg_NL : concentration of nongspecific signaling complexes

M_VPA = 144.211;            %molar mass VPA (g/mol)
V0_init = logspace(log10(Vbounds(1)),log10(Vbounds(2)),20);
V0 = ((V0_init./M_VPA)*(10^-3))./DF;
A0 = Am0 / v_as;
C0 = Cm0 / v_as;

%Parameters
%Antibody-VPA binding values
konV = K(1);        %(M^-1s^-1)
KdV= K(2);          % M
koffV = KdV*konV;
%Antibody-conjugate binding values
konC = K(3);
KdC = K(4);
koffC = KdC*konC;
%SB-LB binding values
konNL = K(5);
KdNL = K(6);
koffNL = KdNL*konNL;

endTime = tspan;
tInt = 1e-4;
time = tInt:tInt:endTime;

radius = 5; %(nm)
loc_vol = 4/3*pi*(radius)^3*10^-24; %(L)
N_A = 6.02214076*10^23; %Avogadro's constant (molecules per mol)
effect_C = 1/(loc_vol*N_A); %mol/L

if KdNL <= 1e-6
    p_NL1 = 0.0030/0.0032;
elseif KdNL == 1e-5
    p_NL1 = 0.0029/0.0032;
elseif KdNL == 1e-4
    p_NL1 = 0.0027/0.0032;
end

for ii=1:length(V0)

    A_init = A0;
    C_init = C0;
    V_init = V0(ii);
    AC_init = 0;
    AV_init = 0;
    C_AC_init = 0;
    C_AV_init = 0;
    C_A_init = 0;
    NL_init = 0;


    A = [A_init,zeros(1,length(time)-1)];
    C = [C_init,zeros(1,length(time)-1)];
    V = [V_init,zeros(1,length(time)-1)];
    AC = [AC_init,zeros(1,length(time)-1)];
    AV = [AV_init,zeros(1,length(time)-1)];
    C_A = [C_A_init,zeros(1,length(time)-1)];
    C_AC = [C_AC_init,zeros(1,length(time)-1)];
    C_AV = [C_AV_init,zeros(1,length(time)-1)];
    NL = [NL_init,zeros(1,length(time)-1)];
    all_NL = [0, zeros(1,length(time)-1)];

    tstep = 1;

    for i = 1:(length(time)-1)
        dAdt = koffC*AC(tstep)-konC*A(tstep)*C(tstep) + koffV*AV(tstep)-konV*V(tstep)*A(tstep) + koffNL*C_A(tstep)-konNL*C(tstep)*A(tstep);
        dCdt = koffC*AC(tstep)-konC*C(tstep)*A(tstep) + koffNL*C_AC(tstep)-konNL*AC(tstep)*C(tstep) +
konC*C_A(tstep)*C(tstep)-koffC*C_AC(tstep) + koffNL*C_AV(tstep)-konNL*AV(tstep)*C(tstep);
        dVdt = koffV*AV(tstep)-konV*A(tstep)*V(tstep) + koffV*C_AV(tstep)-konV*C_A(tstep)*V(tstep);
        dACdt = konC*A(tstep)*C(tstep)-koffC*AC(tstep) + koffNL*C_AC(tstep)-konNL*AC(tstep)*C(tstep);
        dAVdt = konV*A(tstep)*V(tstep)-koffV*AV(tstep) + koffNL*C_AV(tstep)-konNL*AV(tstep)*C(tstep);
        dC_Adt = konNL*C(tstep)*A(tstep)-koffNL*C_A(tstep) + koffC*C_AC(tstep)-konC*C_A(tstep)*C(tstep)
+koffV*C_AV(tstep)-konV*C_A(tstep)*V(tstep);
        dC_ACdt = konNL*AC(tstep)*C(tstep)-koffNL*C_AC(tstep) + konC*C_A(tstep)*C(tstep)-koffC*C_AC(tstep);
        dC_AVdt = konNL*AV(tstep)*C(tstep)-koffNL*C_AV(tstep) + konV*C_A(tstep)*V(tstep)-koffV*C_AV(tstep);

        A(tstep+1) = dAdt*tInt + A(tstep);
        C(tstep+1) = dCdt*tInt + C(tstep);
        V(tstep+1) = dVdt*tInt + V(tstep);
        AC(tstep+1) = dACdt*tInt + AC(tstep);
        AV(tstep+1) = dAVdt*tInt + AV(tstep);
        C_A(tstep+1) = dC_Adt*tInt + C_A(tstep);
        C_AC(tstep+1) = dC_ACdt*tInt + C_AC(tstep);
        C_AV(tstep+1) = dC_AVdt*tInt + C_AV(tstep);

        NL(tstep+1) = AC(tstep)*p_NL1 + C_A(tstep);
        %all_NL(tstep+1) = C_A(tstep+1) + C_AC(tstep+1) + C_AV(tstep+1) + NL(tstep+1);

        tstep = tstep+1;
```

```
    end
data(:,:,ii) = [A; C; V; AC; AV; C_A; C_AC; C_AV; NL]'.*1e9;

end
  output = (reshape(data(size(data,1),:,:),[size(data,2) 20]))'; %take the last time point

  pos_NL = output(:,9);
  neg_NL = output(:,6)+output(:,7)+output(:,8);
end
```

Grey Relational Analysis

```
%% PART 1: DESIGN OF EXPERIMENT
% { inputs details } %
in_names = ["A0 (mol)"; "C0 (mol)"; "Assay volume(L)"; "Dilution factor"; "Assay time";"NanoLuc dissociation constant"];
in_A     = [1e-17 1e-15 1e-13];
in_C     = [1e-15 1e-13 1e-11];
in_vol     = [1e-7 1e-6 1e-5];
in_DF     = [1 10 100];
in_t     = [10 20 30];
in_K = [1e-7 1e-6 1e-5 1e-4];
in_table = table(in_A, in_C, in_vol, in_DF, in_t, in_K);

% { outputs details } %
out_names   = ["Linearity error"; "median signal"; "range"; "CV(15)"];

%% PART 2: RESERVE MEMORY
% creates experiment setup
in_nr = length(in_names);
out_nr = length(out_names);
%out_coef = out_coef * ones(out_nr, 1);
fullfact_size = zeros(1, in_nr);

for i = 1:in_nr
    fullfact_size(i) = size(table2array(in_table(:,i)),2);
end
dof = fullfact(fullfact_size);

% reserves memory for results
dof = [dof zeros(length(dof), 3 * out_nr + 2)];
%
i_expr = in_nr+1:in_nr+out_nr;


%% PART 3: RUN EXPERIMENTS
V0 = [4 15]; %(fVPA) range of VPA initial sample concentration (ug/mL)
for i = 1:size(dof,1)
    K = [1e5 1e-8 1e5 1e-8 5e2 in_K(dof(i,6))];
    [pos_NL(i,:), neg_NL(i,:)] = VPA_Assay_run(V0,in_A(dof(i,1)),in_C(dof(i,2)),in_vol(dof(i,3)),in_DF(dof(i,4)),in_t(dof(i,5)),K);
end
NL_total = pos_NL + neg_NL;

% OUTPUT FEATURES
% Linearity
x = logspace(log10(V0(1)),log10(V0(2)),20);
a = 1/(log10(V0(1))-log10(V0(2)));
b = -a*log10(V0(2));
y_ideal = log10(x)*a+b;
D = max(NL_total,[],2) - min(NL_total,[],2);
ynew = ((NL_total - min(NL_total,[],2))./D);
sqerror = sum((ynew-y_ideal).^2,2); %minimize (7)

% Median signal
med_sgn = (max(NL_total,[],2)+min(NL_total,[],2))./2;  %maximize (8)

% Signal intensity range
rel_slope = D./((max(NL_total,[],2)+min(NL_total,[],2))/2); %maximize (9)

% Low FP / TP
background = mean(neg_NL,2);
CV = neg_NL(:,end)./NL_total(:,end); %minimize (10)

dof(:,i_expr) = [sqerror,log10(med_sgn),rel_slope,CV];

%% PART 4: GREY RELATIONAL ANALYSIS
out_names   = ["Linearity error"; "median signal"; "range"; "CV(15)"];
out_optimal = ["low", "high", "high", "low"]; % low, high, norm (= target)
out_norm = [0, 0,0, 0]; % target for norm optimal, use 0 for low and high
out_weights = [1 1 1 1]./4;
out_coef    = 0.5;
out_coef = out_coef * ones(out_nr, 1);

% indexes
i_inpt = 1:in_nr;
i_norm = in_nr+out_nr+1:in_nr+2*out_nr;
i_coef = in_nr+2*out_nr+1:in_nr+3*out_nr;
i_grad = in_nr+3*out_nr + 1;
i_rank = in_nr+3*out_nr + 2;

% normalize, weighted sum and rank
for i = 1:out_nr
    dof(:,i_norm(i)) = gra_norm(dof(:,i_expr(i)), out_optimal(i), out_norm(i));
    dof(:,i_coef(i)) = gra_coef(dof(:,i_norm(i)), out_coef(i));
end
dof(:,i_grad) = dof(:,i_coef) * out_weights';
dof = sortrows(dof,i_grad);
dof(:,i_rank) = transpose(1:size(dof,1));

% input response table, and create plot
input_response = gra_input_response(dof, in_nr, i_grad, in_names);
%%
gra_plot(in_table, input_response, in_nr, in_names);

% converts the result matrix into a table
```

```
labels = {compose('%s', in_names); compose('%s', out_names);
          compose('normalized %s', out_names);
          compose('GR_Coef %s', out_names); {'GR_Grade'}; {'rank'}};
dof = array2table(dof, 'VariableNames', cat(1, labels{:}));


%% PART A: APPENDIX FUNCTIONS
function norm = gra_norm(x, x_value, target)
    if (x_value == "high")
        norm = (x(:)-min(x))./(max(x) - min(x));
    end
    if (x_value == "low")
        norm = (max(x)-x(:))./(max(x) - min(x));
    end
    if (x_value == "norm")
        norm = 1 - abs(x(:)-target) ./ max(max(x)-target, target - min(x));
    end
end

function coef = gra_coef(x, x_coef)
    coef = (x_coef * max(x))./(x_coef * max(x) + (1 - x(:)));
end

function gra_rank = gra_sort(x)
    gra_rank = zeros(0,length(x));
    [sorted, ~] = sort(x, 'descend');
    for i = 1:length(sorted)
        gra_rank(i) = find(sorted==x(i));
    end
end

function result = gra_input_response(x, in_nr, i_grad, inputs)

    levels = NaN(in_nr, max(max(x(:,1:in_nr))));
    effect = zeros(in_nr,1);
    rank = zeros(0,length(x));

    for input = 1:in_nr
        for level = 1:max(x(:,input))
            levels(input, level) = mean(x(x(:,input) == level,i_grad));
        end
        effect(input) = max(levels(input,:)) - min(levels(input,:));
    end

    rank = gra_sort(effect(:,end));
    rank = transpose(rank);
    result = table(inputs, levels, effect, rank);
end

function gra_plot(in_table, input_response, in_nr, in_names)

    figure('Name','Grey Relational Input Response','NumberTitle','off')
    for i = 1:in_nr
        subplot(1,in_nr,i);
        x = table2array(in_table(:,i));
        y = table2array(input_response(i,2));
        semilogx(x,y(~isnan(y)), '-*', 'LineWidth',2);
        axis tight
        ylim([0 1]);
        title(in_names(i));
        if (i == 1)
            ylabel('Grey Relational Grade')
        end
    end
end
```

Enzyme kinetics

```
s0=10*10^-6;
e0=2.2104902047479*10^-9;
p0=0;
es0=0;
Na=6.02214e23;
rd=0.002;
Nq=0.3;
A_detection=4.8*10^-6;
Res=0.1;

x0 = [s0 e0 p0 es0];
tspan = [0 10];
opts = odeset('RelTol',1e-14,'AbsTol',1e-14);
[t,x] = ode45(@enzymreaction,tspan,x0,opts); %Runge-Kutta

ii=1;
flux=[];
while ii<length(t)
    flux(ii)=(x(ii+1,3)-x(ii,3))./((t(ii+1)-t(ii)));
    ii=ii+1;
end
flux(length(flux)+1)=flux(length(flux));
flux=transpose(flux);
flux=max(0,flux);
nrPhoton=floor(flux*Na*Nq);
nrPhoton=(nrPhoton./(4*pi*rd^2));
E_photon=((3*10^8)*(6.6*10^-34))/(429*10^-9);
Energyflux=nrPhoton.*E_photon;
Wattage=Energyflux.*A_detection;
Current=Res*Wattage;

figure,plot(t,Current*10^3)
ylabel('Current (mA)');
xlabel('Time (s)');
```

```
function [f]=enzymreaction(t,x)

s=x(1);
e=x(2);
p=x(3);
es=x(4);

kf=10^9;
kr=2*10^-1;
kcat=9*10^1;

f(1)=-kf*e*s+kr*(es);
f(2)=-kf*e*s+kr*(es)+kcat*(es);
f(3)=kcat*(es);
f(4)=kf*e*s-kr*es-kcat*es;

f=f(:);
end
```

Appendix H Survey Kempenhaeghe

Als studententeam van de Technische Universiteit Eindhoven (TU/e) zijn wij op dit moment bezig met het ontwikkelen van een biosensor voor anti-epileptica, met de nadruk op Valproaat: een apparaat dat snel, makkelijk en vaak de bloedconcentratie gehaltes van de medicijnen kan meten. Met deze biosensor doen wij mee aan de SensUs competitie in augustus 2020 waarbij meerdere teams over heel de wereld mee doen en hun biosensor aan de rest van de deelnemers laten zien. Om erachter te komen waar op dit moment de valkuilen en verbeteringen liggen bij de huidige anti-epileptica therapieën hebben we hulp nodig van ervaringsdeskundigen. Deze input kunnen wij dan gebruiken om onze biosensor aan te passen en toe te kunnen passen om hopelijk problemen op te lossen die er nu zijn. Daarom vragen wij u de volgende vragen in te vullen. Mocht u een vraag niet willen beantwoorden of het antwoord niet weten, dan kunt u de vraag leeg laten. De informatie verkregen uit deze vragenlijst blijft anoniem en zal uitsluitend voor intern gebruik zijn.
Wat is uw leeftijd?

Wat is uw geslacht?

- o Man
- o Vrouw
- o Anders
- o Zeg ik liever niet

Vraag 1. Anti-epileptica
De volgende vragen gaan over het gebruik van uw voorgaande en huidige anti-epileptica.

A) Welke van de volgende anti-epileptica gebruikt u momenteel? Meerdere antwoorden kunnen aangekruisd worden.

- o Brivaracetam
- o Carbamazepine en oxcarbazepine
- o Clobazam
- o Fenytoïne
- o Gabapentine
- o Lacosamide
- o Lamotrigine
- o Levetiracetam
- o Perampanel
- o Pregabaline
- o Topiramaat
- o Valproaat
- o Zonisamide
- o Anders:

B) Bent u tevreden over uw huidige anti-epileptica?

- o Ja
- o Nee

C) Waarom bent u wel/niet tevreden over uw huidige anti-epileptica? Denk hierbij aan eventuele bijwerkingen van het medicijn.

D) Welke van de volgende anti-epileptica heeft u in het verleden gebruikt? Meerdere antwoorden kunnen aangekruisd worden.

- o Brivaracetam
- o Carbamazepine en oxcarbazepine
- o Clobazam
- o Fenytoïne
- o Gabapentine
- o Lacosamide
- o Lamotrigine
- o Levetiracetam
- o Perampanel
- o Pregabaline
- o Topiramaat
- o Valproaat
- o Zonisamide
- o Anders:

E) Waarom bent u overgestapt op andere anti-epileptica? Indien u geen antwoord had aangekruist kunt u deze vraag overslaan.

F) Gebruikt u andere medicijnen naast anti-epileptica?

- o Ja
- o Nee

G) Vergeet u wel eens om uw medicatie in te nemen?

- o Ja
- o Nee
- o Zeg ik liever niet

H) Zo ja, hoe vaak komt dit voor?

- o Om de dag
- o Wekelijks
- o Maandelijks
- o Eens per jaar
- o Anders:

I) Indien van toepassing, wat was de voornaamste reden dat u uw medicatie vergat?

Vraag 2. Bloedspiegelbepaling

A) Heeft u recentelijk of in het verleden een bloedspiegelbepaling voor anti-epileptica ondergaan?

- o Ja
- o Nee

B) Indien u "Ja" op vraag 2A heeft geantwoord: Hoe vaak heeft u afgelopen jaar bloedspiegels moeten laten controleren?

- o Iedere dag
- o Iedere week
- o Iedere maand
- o Ieder half jaar
- o Nooit
- o Anders:

C) Indien u "Ja" op vraag 2A heeft geantwoord: Was de bloedspiegelbepaling thuis of in het ziekenhuis?

- o Thuis
- o Ziekenhuis

D) Indien u "Ja" op vraag 2A heeft geantwoord: Wat was uw ervaring bij de bloedspiegelbepaling ?

- o 1 Heel positief
- o 2
- o 3
- o 4
- o 5 Heel negatief

E) Indien negatief, welke ervaring(en) vond u negatief?

Vraag 3. Biosensor en bloedafname
Een biosensor is een klein apparaat bij u thuis die de bloedspiegel van bijvoorbeeld medicijnen bepaalt. Hierbij word eerst bloed afgenomen en vervolgens door middel van de biosensor geanalyseerd; denk hierbij aan het voorbeeld van een glucose meter die wordt gebruikt wordt door patiënten met diabetes. De biosensor is bedoeld om meerdere keren per week uw bloedspiegel te bepalen en is daarom bedoeld om gemakkelijk en snel bij u thuis te kunnen meten. Uw mening als patiënt en potentieel gebruiker is daarom van belang om de toegevoegde waarde van een biosensor te achterhalen en op welke manier deze het beste kan worden toegepast.

A) Bent u bekend met biosensoren?

- o Ja
- o Nee

B) Heeft u in het verleden gebruik gemaakt van een dergelijke biosensor? Denk hierbij bijvoorbeeld aan een glucose meter.

- o Ja
- o Nee

C) Indien u "Ja" op vraag 3B heeft geantwoord: Moest u bij het gebruik van een dergelijke biosensor zelf bloed afnemen? Denk hierbij aan een vingerprik.

- o Ja
- o Nee

D) Indien u "Ja" op vraag 3C heeft geantwoord: Hoe zou u uw ervaring bij deze bloedafname beschrijven?

- o 1 Absoluut geen probleem
- o 2
- o 3
- o 4
- o 5 Een erg groot probleem

E) Indien u geen ervaring heeft met het zelf afnemen van bloed, bent u bereid om zelf bloed af te nemen in de vorm van een vingerprik als dit nodig is voor het gebruik van een dergelijke biosensor?

- o Ja
- o Nee

Indien u "Nee" op vraag 3E heeft geantwoord: Kunt u toelichten waarom u niet een bloedprik bij uzelf uit zou willen voeren?

Vraag 4. Overige problemen

A) Zijn er op dit moment verder problemen omtrent de behandeling van epilepsie?

- o Ja
- o Nee

B) Zo ja, kunt u deze problemen toelichten?

C) Indien van toepassing, heeft u suggesties voor oplossingen voor deze problemen die u wellicht ook al met uw arts or specialist besproken heeft?

Het einde van de enquête

Dit is het einde van de vragenlijst. Bedankt voor uw samenwerking! Mocht u vragen en/of opmerking hebben dan kunt u ons altijd bereiken op teamtest@tuetest.nl.